Comparison of LES, RANS and Experiments in an Aeronautical Gas Turbine Combustion Chamber

Boudier G.[⋆], Gicquel L. Y. M.[⋆], Poinsot T.[⋆,†]

Bissières D.[‡] and Bérat C.[‡]

May 9, 2006

[⋆] CERFACS, 42 Avenue G. Coriolis, 31057 Toulouse cedex, France

[†] Institut de Mécanique des Fluides de Toulouse, Avenue C. Soula, 31400 Toulouse, France

[‡] Turbomeca, Safran group, 64511 Bordes cedex, France

Corresponding author:

Guillaume Boudier

CERFACS - 42 Avenue Coriolis

31057 TOULOUSE CEDEX FRANCE

FAX: +33 5 61 19 30 00 - EMAIL: boudier@cerfacs.fr

Colloquium: 11. IC Engines and Gas Turbine Combustion

Short title: LES, RANS and Experiment for Exit Temperature

Total number of pages: 16

Total length of paper: 4970 words (Method 2)

Listing of word count: Main text (3009) Equations (73) References (335) Figures (1:189, 2:123, 3:121, 4:165, 5:268, 6:106, 7:224, 8:123, 9:119, 10:115)

Abstract: Although Large Eddy Simulations (LES) have demonstrated their potential in simple academic combustion chambers, their application to real gas turbine chambers requires specific developments and validations. In this study, three specific aspects of such chambers are discussed: multiple inlets, multi-perforated plates and film cooling. LES is used in an industry-like chamber and results are compared with predictions provided by Reynolds Averaged Navier-Stokes (RANS) simulations and experimental measurements. Multi-perforation is handled using a simplified effusive wall law while film cooling makes use of low resolution influx conditions ('coarse LES'). Experimental results are well reproduced and qualitatively improved when compared to RANS predictions. LES results underline the potential of the approach for industrial use.

Keywords: Combustion; Aeronautical Gas Turbine; Large Eddy Simulations

1 Introduction

Many recent Large Eddy Simulations (LES) have demonstrated the potential of LES in reasonably simple academic combustion chambers. For such configurations, LES provide excellent evaluations of mean and Root Mean Square (RMS) fields of temperature, species and velocities [1–10]. It also allows to investigate the unsteady structures in such flows [1–4] which can lead to instabilities known to be critical in many industrial programmes.

Despite these successes, the path for LES to become a validated production tool in the gas turbine industry is still unclear. Indeed, for this tool to properly enter the design steps of the next generation of aeronautical gas turbines, industrial requirements have to be met. In this study, the following issues are considered:

- Real combustion chambers contain specific elements which are not found in most laboratory burners. The first one is the existence of multi-perforated plates used for wall cooling. These plates contain thousands of small holes (less than 1 mm in diameter) which cannot be resolved individually. The second one is the use of multiple cooling films having thicknesses (about 1 mm) too small for standard LES grids. An additional theoretical issue is that while academic combustion chambers are generally limited to fully premixed or fully non-premixed regimes, fuel and air are injected in real gas turbines chambers through multiple inlets making certain models difficult to use. Defining a unique mixture fraction, for example, becomes difficult in a real engine where multiple streams of different temperatures and concentrations feed the combustion chamber. Performing LES in such chambers therefore needs specific models.

- Even though LES has shown promising results in the near-injector zone of burners, the first criterion used daily by gas turbine manufacturers is the proper prediction of the chamber exit mean temperature profile because it is a key design parameter of the turbine specification. Large spatial variations of the mean temperature field prior to the turbine lead to shortened engine life-times. A key question for industry is therefore to know whether LES produces better results for chamber exit temperatures than RANS (Reynolds Averaged Navier-Stokes) methods used today.

Of course, it is expected that better results near the injectors will also mean better predictions for outlet temperatures, but this is not necessarily so. Indeed, the two previous issues are linked: if multi-perforation and film cooling are not properly accounted for, mixing of the fresh gases issued by these cooling systems with the hot products of combustion will not be properly predicted and heterogeneities in the exit mean temperature profiles will not be properly reproduced. Of course, if the combustion model is not adapted to multiple inlet combustion regimes, the temperature field will also be inaccurate.

In this paper, LES is used on a complex gas turbine chamber including multi-perforated plates and film cooling. Specific sub-models are developed for these cooling devices. A combustion model using a two-step chemical mechanism for n-decane coupled to the thickened flame model [1, 2] is used in a compressible LES solver [11]. The flame structure is analyzed using LES data and the outlet temperature profiles obtained with LES are compared to RANS and experimental data provided by Turbomeca (Safran group).

The organisation of the paper is as follows: first a brief review of the LES code is given, followed by a short presentation of models employed and the chemical scheme developed. Details of the combustion chamber are then exposed along with the various flow parameters necessary for LES: grid, boundary conditions. LES results are then produced and qualitatively compared to RANS predictions. Specific attention is devoted to the exit mean temperature distributions for which RANS and experimental data are available.

2 Numerical approach used in Large Eddy Simulations

The LES solver uses a finite-volume discretization of the fully compressible multi-species (variable heat capacities) Navier-Stokes equations. It is able to handle fully unstructured / structured / hybrid meshes. Higher order temporal and spatial schemes [11, 12] offer reliable unsteady solutions for complex geometries as encountered in the field of aeronautical gas turbines.

2.1 LES closures for turbulent stresses

The concept of LES introduces the notion of spatial filtering to be applied to the set of governing equations used to simulate turbulent reacting flows [13, 14]. Resulting from this operation are unclosed terms issued from the non-linear character of the Navier-Stokes equations. To solve numerically the filtered Navier-Stokes equations, Sub-Grid Scale (SGS) models need to be supplied to mimic the turbulent scale effects on the resolved field [15].

In this work, SGS stresses are described using the classical Smagorinsky model [16]. When dealing with wall-bounded flows, wall functions are introduced and yield results comparable to the dynamic model [17]. SGS turbulent mixing appearing in the species and temperature transport equations are modelled through the gradient hypothesis along with the turbulent Schmidt and Prandtl numbers.

2.2 Reduced scheme for n-decane / air flames

Predictions of exit temperature levels impose the use of precise chemical schemes to correctly predict the flame position. Here a two-step scheme for gaseous n-decane ($nC_{10}H_{22}$) was developed to take into account carbon dioxide (CO_2) dissociation:

$$nC_{10}H_{22} + \frac{21}{2}O_2 \quad \rightarrow \quad 10CO + 11H_2O \tag{1}$$

$$CO + \frac{1}{2}O_2 \quad \rightleftharpoons \quad CO_2 \tag{2}$$

The first reaction, Eq. (1), is irreversible and decomposes the complex hydrocarbon into carbon monoxide (CO) and water (H_2O). The second reaction, Eq. (2), is the re-combination of the carbon monoxide in carbon dioxide and essentially aims at controlling the heat release issued by the first reaction. It is designed to be an equilibrium process.

Reaction constants such as the pre-exponential constants have been fitted using CHEMKIN along with a detailed chemical scheme containing 91 species and 1328 reactions (Turbomeca private communication).

Figure 1 shows equilibrium temperatures and flame speeds as obtained by the fitted reduced two-step scheme and compared to the detailed mechanism for fully premixed laminar flames. Although differences appear for rich mixtures, the agreement between reduced and full scheme is good for all equivalence ratios below 1.2. In the present case, the overall equivalence ratio of the gas turbine chamber is roughly 0.33 and the maximum equivalence ratio is found in the fuel injector: it is roughly 3.5 but decreases very rapidly in the chamber so that the two-step scheme is considered adequate for the present exercise.

2.3 Subgrid-scale model for flame / turbulence interaction

Flame / turbulence interaction is modelled using the Dynamically Thickened Flame (DTF) approach [18] which allows to handle both mixing and combustion. An important advantage of this model which solves individually for the mass fractions of nitrogen and of all five species involved in reactions 1 and 2 is that it does not make any assumption on the flame regime. Multiple inlets can be used with various temperatures and compositions. Even if a mixture fraction cannot be properly defined, the DTF model can still be used as it solves explicitely for all species and reaction rates. The model has been tested elsewhere in various configurations [1, 19–21]. Issues pertaining to the potential limitations of the DTF model [18] are acknowledged at this point and need investigation for diffusion flames. This specific subject is believed to be outside the scope of this particular work which is devoted to the assessment of LES in real gas turbine engines.

3 Target configuration

3.1 Chamber characteristics

The computational domain is a 36 degree section of an annular inverted-flux combustion chamber designed by Turbomeca (Safran Group). A premixed gaseous mixture of n-decane enters the chamber through a pre-vaporizer (Fig. 3). Fresh gases are consumed in the primary zone, delimited by the chamber dilution holes and the end wall of the combustion chamber (Fig. 2). To ensure full combustion, this region of the chamber is fed with air by primary jets located on the inner liner (Fig. 2). Burnt gases are then cooled in the remaining part of the combustor thanks to dilution holes or cooling films located on the inner and outer liners as well as on the return bend of the combustion chamber. Multi-perforated plates ensure local wall cooling in a restricted area of the chamber as shown on Fig. 2.

3.2 Numerical characteristics

LES of the reacting flow are conducted for an unstructured mesh composed of $286,500$ nodes and $1,550,000$ tetrahedric elements resulting in an explicit time step of about $0.13\mu s$. The mesh is refined in the vicinity of the pre-vaporizer outlets, the primary holes and the dilution holes, to provide a proper representation of the premixed combustion process. Special attention is devoted to the grid spacing in the region of films to ensure a manageable time step. In general, the height of the film inlets is represented by one face of a single element which imposes the manipulation of the fluxes through this face to specify the boundary conditions (BCs). The same approach is used for the specification of the cooling air effusing from the multi-perforated walls. These walls are also 'homogeneized': the flow issuing from the perforation jets is distributed over the whole surface and corrections are performed for momentum and turbulent law-of-the-walls to account for these jets. The other inlet and outlet BCs are treated with the Navier-Stokes Characteristic Boundary Conditions (NSCBC) [11, 22] to control the acoustic behaviour of the system. Side boundaries are considered axi-periodic. The operating point is the same for LES, RANS and experiment and corresponds to the cruising operating point.

RANS computation is performed on a half sector unstructured mesh composed of $150,000$ nodes and $825,000$ tetrahedras. Side boundaries are symmetries.

4 Results and discussions

This section presents instantaneous LES temperature fields to illustrate the unsteady nature of the flow. Assessment of the mean temperature field and exit mean temperature profile is obtained by comparisons against RANS results as well as experimental measurements. Planes of interest are identified on Fig. 4. Radial variations of the mean temperature field obtained near the exit of the chamber, plane 3 of Fig. 4, are also investigated.

4.1 Unsteady LES temperature fields

Figure 5 shows instantaneous temperature fields scaled by the inlet temperature within the combustion chamber in three planes identified on Fig. 4.

Fresh gases exiting from the pre-vaporizer are burnt through a rich premixed flame attached to the pre-vaporizer outlet sections (see Fig. 5b). The remaining unburnt gases, composed of pure n-decane mixed with combustion products, are consumed by diffusion flame fronts located near the chamber head cooling films and the primary holes.

Combustion is restrained to the primary zone of the chamber as designed initially by Turbomeca. Primary holes feed the diffusion flame with oxygen, Fig. 5b, while dilution holes confine the chamber's primary region, Fig. 5a, by dramatically cooling the hot gas mixture. Note that these latter holes partially contribute to combustion by adding oxygen to the reacting zone. Cooling films clearly contribute to the wall cooling process by shielding the liners from the hot gases. More specifically, the outer chamber head cooling film pushes the hot gases within the inner part of the combustor and contributes to the combustion. Instantaneous temperature fields are displayed on Fig. 5c for the plane where the experiment was performed. At this location, cool and hot air are still partially segregated: hot gases tend to concentrate in the upper part of the section. A significant decrease in the peak temperature is however achieved when compared to the instantaneous fields going through the entire combustion chamber, Figs. 5a and 5b.

LES results also provide insights into the regime at which combustion locally takes place: Fig. 6 displays a Probability Density Function (PDF) of local equivalence ratio for all points in the chamber where a significant heat release takes place. Two peaks are observed: at 0.6 (the lean flammability limit) and 1 (stoichiometry). Very few flame elements burn in very rich conditions, thereby justifying to first order the use of a two-step chemical mechanism.

LES is seen to produce temporal and spatial evolutions of this highly unsteady reacting flow which constitutes a valuable information for design purposes. Assessment of the predictions in terms of industrial criteria is however still needed. This is the aim of the following section where mean temporal LES predictions are gauged against RANS results and experimental measurements.

4.2 Validation of the LES mean temperature predictions

Mean temporal values of the LES temperature fields are obtained through Reynolds average of the instantaneous LES predictions. Integration is here performed for roughly four flow-through times to ensure convergence of the first moments. Figures 7 and 8 depict the mean temperature fields scaled by the inlet temperature obtained by LES and RANS for the same configuration. Mean temperature distributions in the various planes of interest are much sharper in LES and reacting regions reach larger temperature values when compared to RANS. Such differences are explained through the theoretical differences inferred by the two approaches and the well known smearing effect of RANS modelling. Note that a classical $k - \varepsilon$ model is used for RANS turbulence closure. The RANS turbulent combustion model is the Cramer Limited by Equilibrium (CLE) model [23] corresponding to a mixed-is-burnt model limited by equilibrium. Modelling differences between RANS and LES easily explain the different flame positions when comparing the two methods. If identified by the peak of the mean temperature, the LES mean flame front essentially encompasses most of the primary zone of the combustor. RANS predict an overall longer flame front spreading beyond the primary holes. Very few studies have addressed the comparison of RANS and LES methods for reacting flows in complex configurations. Figure 7 shows that there are very significant differences. Among them is the discrepancy observed in the near-field of the injector and especially on the dilution jet trajectories. In general, LES jet penetrations are less pronounced than the one obtained with RANS. These variations are expected to be major sources of differences when assessing the mean exit temperature profiles since dilution jets are the primary source of temperature heterogeneities in the tail of the combustor. These near-injectors differences between RANS and LES results are somewhat damped as the flow moves downstream and mixing takes place. However even the mixing is computed differently in both approaches, significant differences exist betwen RANS and LES (Fig. 8).

These differences can be assessed by a parameter (called here $RTDF$ for Radial Temperature Distribution Function) which measures the temperature heterogeneities in a plane upstream of the turbine. The primary aim of this parameter is to quantify the radial evolution of the mean azimuthal temperature variations from the mean planar value. If r and θ refer to the radial and the azimuthal coordinates, the analytical expression of this industrial design parameter reads:

$$RTDF(r) = \frac{< \overline{T}(r,\theta) >_{\theta} - < \overline{T}(r,\theta) >_{\theta r}}{< \overline{T}(r,\theta) >_{\theta r} - \overline{T}_{in}}, \qquad (3)$$

where $< \overline{T}(r,\theta) >_{\theta}$, $< \overline{T}(r,\theta) >_{\theta r}$ and $\overline{T}_{in}$ are respectively the mean azimuthal temperature, the mean planar temperature and the mean chamber inlet temperature. The notations $\overline{f}, < f >_{\theta}$ and $< f >_{\theta r}$ respectively refer to the temporal mean of f, its azimuthal mean and its planar mean.

$RTDF(r)$ quantifies the degree of heterogeneity seen by the turbine blades and needs to be controlled because of mechanical and thermal constraints. Mixing of the cool gases with the hot products issued from the combustion zone is henceforth critical to properly predict this quantity. $RTDF(r)$ for plane 3 obtained from LES and RANS is shown on Fig. 9 (black lines) along with experimental measurements derived from four radial positions on the real engine (open diamonds) and their associated error bars.

The agreement between measured data and LES results is very encouraging. LES prediction of this design criterion better reproduces the experimental trend when compared to RANS which, in itself, constitutes a valuable asset for LES. Differences in the $RTDF(r)$ profile essentially appear for high values of the radial position. Based on both LES and measurements, hot gases are expected to preferentially concentrate in the upper region of plane 3 as already observed on Fig. 8. LES however do not predict the increased mixing near the walls as illustrated by the measurements. The sensitivity of the $RTDF(r)$ profiles to the averaging time is presented on Fig. 10. Relatives errors introduced by the change of the integration duration (from one to four flow-through times) remain minor.

5 Conclusions

Application of LES to industrial configurations promises to be of great interest for design purposes. Indeed, because of the capacity of the approach to predict unsteady turbulent reacting flows [1–4], LES yield information that is not accessible with conventional numerical approaches. Among the potential mechanisms grasped by LES and of great importance to industry, one retains: flame turbulence interactions, flame acoustic coupling and all the large scale temporally dependent flow features such as mixing. Validation of the approach when applied to industrial configurations is however still needed. In an attempt to assess LES in a real combustion chamber, predictions of the flow within a Turbomeca combustor using LES and RANS was performed in this work. Comparisons against RANS and experimental results underline the differences inferred by the two numerical approaches. In that respect, LES mean temperature fields within the chamber are observed to be sharper and to reach larger values. Assessment of the predictions in terms of the $RTDF(r)$ profile, a design parameter quantifying the mean exit temperature heterogeneities seen by the turbine, proves LES to be very promising and out-performing RANS. Such a statement needs however to be poundered by the relative computer cost of each approach. Today, computer capabilities still remain favorable to RANS especially in the industrial context. Among the numerically important parameters evidenced by this work, one stresses the necessity of dealing with the entire cooling system of the real gas turbine engine. To properly take into account film cooling as well as multi-perforated plates, specific treatment is implemented to reduce computational costs imposed by such geometrical details. The validation of these developments is obtained in light of the quality of the LES predictions for the Turbomeca chamber.

Acknowledgements

The authors gratefully acknowledge the Turbomeca (Safran group) combustion chamber department who largely contributed to this work by making available experimental data and RANS results. Computer support is provided by CERFACS (Toulouse, France) facility and the ”Centre Informatique National de l’Enseignement Supérieur” (CINES) located at Montpellier, France.

References

[1] S. Roux, G. Lartigue, T. Poinsot, *Combust. Flame* 141 (1/2) (2005) 40–54.

[2] L. Selle, L. Benoit, T. Poinsot, F. Nicoud, W. Krebs, *Combust. Flame* 145 (1/2) (2006) 194–205.

[3] A. Giauque, L. Selle, L. Gicquel, T. Poinsot, H. Buchner, P. Kaufmann, W. Krebs, *J. Turb.* 6 (21) (2005) 1–20.

[4] C. Prière, L. Gicquel, P. Gajan, A. Strzelecki, T. Poinsot, C. Bérat, *AIAA Journal* 43 (8) (2005) 1753–1766.

[5] H. Forkel, J. Janicka, *Flow Turb. and Combustion* 65 (2) (2000) 163–175.

[6] H. Pitsch, H. Steiner, *Phys. Fluids* 12 (2000) 2541–2554.

[7] H. Pitsch, L. Duchamp de la Geneste, in: *Proc. Combust. Inst.*, Vol. 29, 2002, pp. 2001–2008.

[8] H. Pitsch, *Ann. Rev. Fluid Mech.* 38 (2006) 453–482.

[9] V. Sankaran, S. Menon, *J. Turb.* 3 (2002) 011.

[10] V. Chakravarthy, S. Menon, *Flow Turb. and Combustion* 65 (2000) 133–161.

[11] V. Moureau, G. Lartigue, Y. Sommerer, C. Angelberger, O. Colin, T. Poinsot, *J. Comput. Phys.* 202 (2005) 710–736.

[12] O. Colin, M. Rudgyard, *J. Comput. Phys.* 162 (2) (2000) 338–371.

[13] S. B. Pope, *Turbulent flows*, Cambridge University Press, 2000.

[14] P. Sagaut, *Large Eddy Simulation for incompressible flows*, Scientific computation series, Springer-Verlag, 2000.

[15] T. Poinsot, D. Veynante, *Theoretical and numerical combustion, second edition*, R.T. Edwards, 2005.

[16] J. Smagorinsky, *Mon. Weather Review* 91 (1963) 99–164.

[17] M. Germano, *J. Fluid Mech.* 238 (1992) 238–325.

[18] J.-P. Légier, T. Poinsot, D. Veynante, in: *Summer Program 2000*, Center for Turbulence Research, Stanford, USA, 2000, pp. 157–168.

[19] L. Selle, G. Lartigue, T. Poinsot, R. Koch, K.-U. Schildmacher, W. Krebs, B. Prade, P. Kaufmann, D. Veynante, *Combust. Flame* 137 (4) (2004) 489–505.

[20] O. Colin, F. Ducros, D. Veynante, T. Poinsot, *Phys. Fluids* 12 (7) (2000) 1843–1863.

[21] Y. Sommerer, D. Galley, T. Poinsot, S. Ducruix, F. Lacas, D. Veynante, *J. Turb.* 5 (2004) 037.

[22] T. Poinsot, S. Lele, *J. Comput. Phys.* 101 (1) (1992) 104–129.

[23] F. Ravet, C. Baudoin, J.-L. Schultz, *Reveue Générale Thermique* 36 (1997) 6–16.

List of Figures

Figures

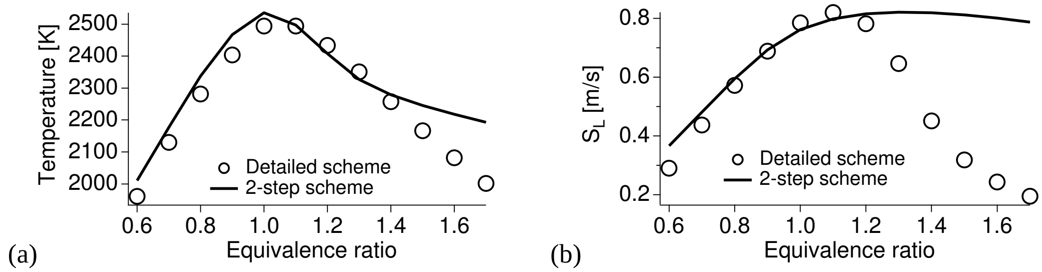

Figure 1: Two-step chemical scheme for n-decane: Validation against the detailed scheme as used in RANS by Turbomeca for (a) the temperature of the burnt gases and (b) the flame speed as functions of the equivalence ratio.

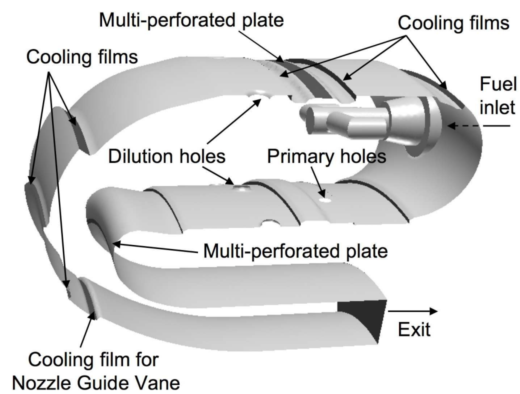

Figure 2: Turbomeca combustion chamber considered for LES in an industrial context.

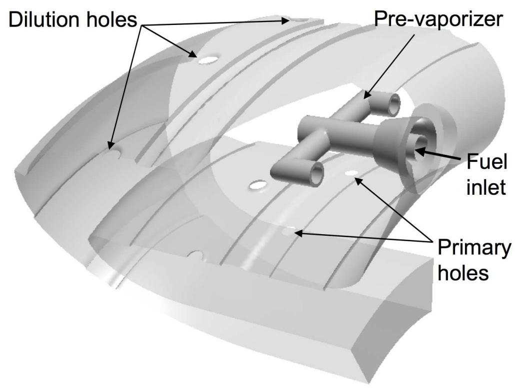

Figure 3: Detailed view of the pre-vaporizer.

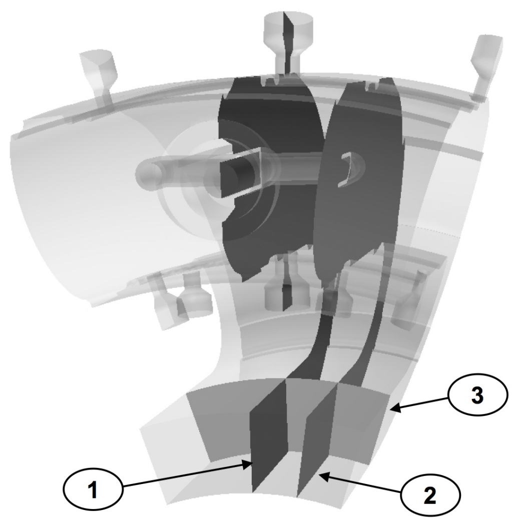

Figure 4: Cutting planes position: 1 Symmetry plane, 2 Pre-vaporizer outlet plane, 3 Plane for temperature measurements in the experiment.

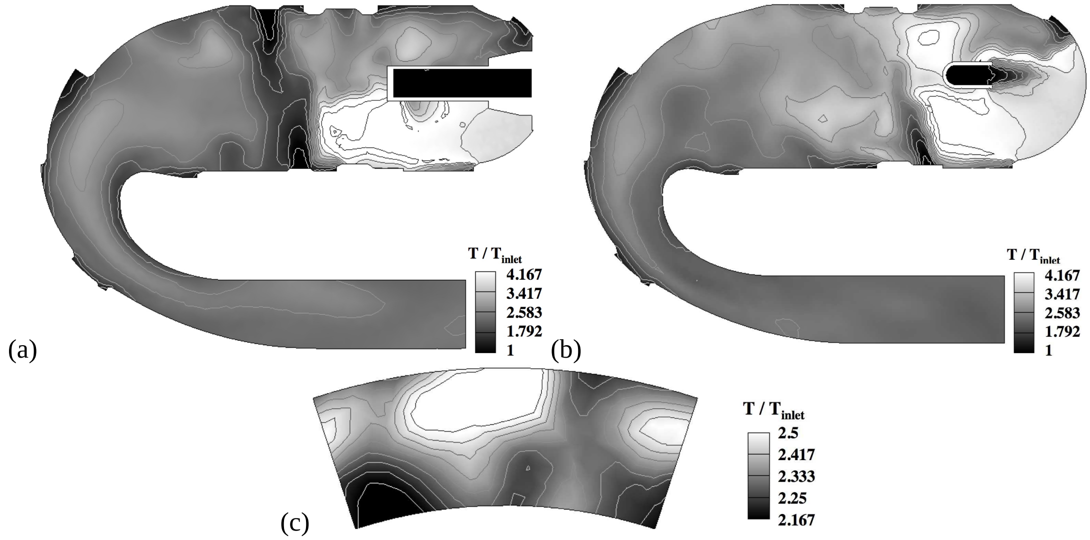

Figure 5: Instantaneous temperature fields T scaled by inlet temperature T_{inlet} as obtained by LES: (a) plane 1, (b) plane 2, (c) plane 3 of Fig.4.

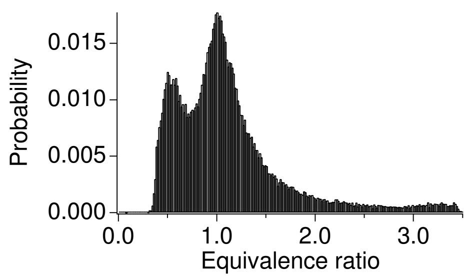

Figure 6: Probability Density Function (PDF) of equivalence ratio in reacting zones.

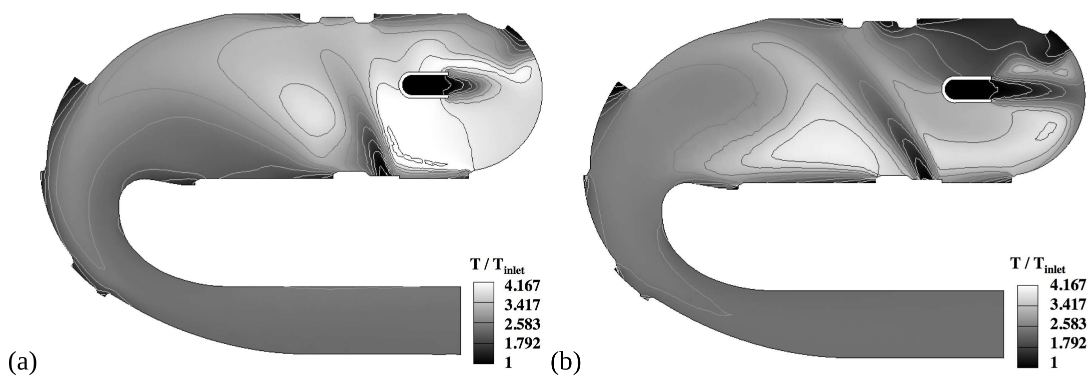

Figure 7: Mean temperature fields T scaled by inlet temperature T_{inlet} as obtained by (a) LES and (b) RANS for plane 2 (*cf.* Fig. 4).

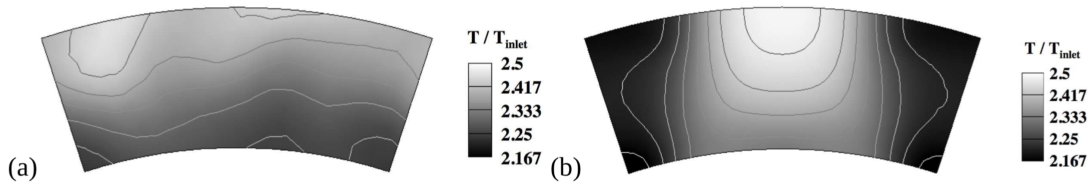

Figure 8: Mean temperature fields T scaled by inlet temperature T_{inlet} as obtained by (a) LES and (b) RANS for plane 3 (*cf.* Fig. 4).

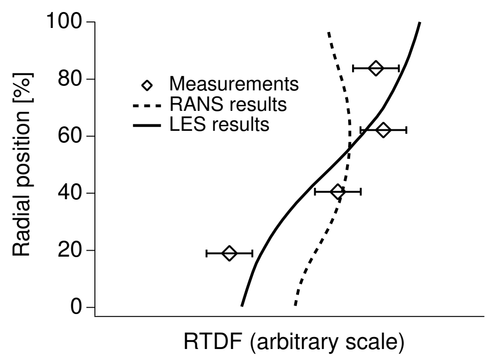

Figure 9: LES and RANS validation in terms of $RTDF(r)$ profile for plane 3 (*cf.* Fig. 4).

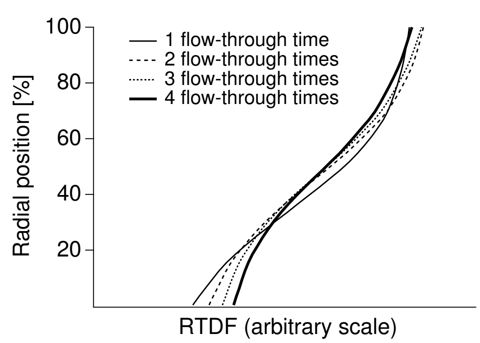

Figure 10: Comparison on $RTDF(r)$ profiles for different integration durations.